Electrical Subharmonic Hybrid Mode Locking of a Colliding Pulse Mode-Locked Laser at 28 GHz

C. Ji, N. Chubun, R. G. Broeke, J. Cao, Y. Du, P. Bjeletich, and S. J. B. Yoo

***Abstract*—This letter discusses electrical subharmonic hybrid mode locking (SHML) of a colliding pulse mode-locked (CPM) laser in InP. The CPM laser fabrication adopts a simple wet etching process and bisbenzocyclobutene planarization process for realizing planarized low-capacitance devices. The experimental results show, for the first time to our knowledge, stable emission of nearly transform-limited pulses at 28 GHz of a CPM laser synchronized to a clock source by SHML. We further describe careful optimization steps of dc and radio-frequency biasing conditions which lead to minimal output pulsewidth of 1.4 ps, limited by the saturable absorber dimension.**

***Index Terms*—Clock synchronization, colliding pulse mode-locked (CPM) laser, radio-frequency (RF) modulation, subharmonic hybrid mode locking (SHML), transform-limited pulse.**

I. INTRODUCTION

SEMICONDUCTOR mode-locked lasers are attractive ultrashort optical pulse sources geared toward integrated microsystem applications for high-capacity optical communication networks such as optical code-division multiple-access networks [1] and ultrafast optical signal processing networks. In particular, colliding pulse mode-locked (CPM) lasers [2]–[4], [6], [8] produce stable and short optical pulses by exploiting saturation effects in the absorber region where two counterpropagating optical pulses collide, while avoiding self-pulsation effects commonly seen in typical mode-locked lasers.

The main shortcoming of passively mode-locked lasers is their large timing jitter and difficulties in synchronization with external clock sources. Two approaches have been demonstrated recently for stabilizing mode-locked lasers. Electrical hybrid mode locking involves radio-frequency (RF) modulations of the gain or the saturable absorber (SA) sections of the mode-locked laser [3]–[5]. Optical synchronous mode locking involves injection of short optical pulses generated by typically another mode-locked laser into the laser cavity [6], [7]. The electrical hybrid mode-locking method is the simpler and more direct approach that requires only an external clock source without additional optical injection setups. In particular, the electrical subharmonic hybrid mode-locking (SHML) technique is a promising approach that requires only an electrical signal at a lower subharmonic frequency as demonstrated in other types of mode-locked lasers [5].

Manuscript received December 27, 2004; revised March 5, 2005. This work was supported in part by Defense Advanced Research Projects Agency (DARPA) and SPAWAR under Agreement N66001-02-1.

The authors are with the Electrical and Computer Engineering Department, University of California, Davis, CA 95616 USA (e-mail: cji@ece.ucdavis.edu; nchubun@ece.ucdavis.edu; rbroeke@ucdavis.edu; jcao@ece.ucdavis.edu; dyixue@ece.ucdavis.edu; bjeletic@ece.ucdavis.edu; yoo@ece.ucdavis.edu).

Digital Object Identifier 10.1109/LPT.2005.848555

This letter discusses SHML operation of an InP CPM laser realized by a self-aligned wet etching fabrication technique. In addition, the epitaxial layers in this laser are designed to facilitate future active–passive device integration. Experimental results include 28.15-GHz CPM laser operation with nearly transform limited optical pulsed output, for the first time, under second-order SHML conditions, and careful optimization procedures leading to CPM laser operation with minimal pulsewidth.

II. MATERIAL COMPOSITION AND DEVICE FABRICATION

The initial wafer for the CPM laser, grown by metal–organic vapor phase epitaxy, consists of, from top to bottom, a 0.1-μm InGaAs contact layer, a 2-μm-thick Zn-doped p-type InP upper cladding layer with a six quantum-well active region, an undoped 0.5-μm-thick InGaAsP waveguiding layer ($1.15Q$) directly below the active region, and a 1.5-μm-thick Si-doped n-type InP lower cladding layer. The active region consists of six 6-nm-wide $In_{0.53}Ga_{0.47}As$ quantum wells separate by 7-nm-wide InGaAsP ($1.25Q$) barriers. The waveguiding layer below the QWs is designed to provide continuous waveguiding of the optical mode across the active–passive interface with low spurious reflections to facilitate future integration of active and passive components [1].

The CPM laser device fabrication started with the deposition of a 150-nm plasma-enhanced chemical vapor deposition SiO_2 layer. Subsequent waveguide definition lithography and reactive ion etching (RIE) etching defined the SiO_2 masking layer for the waveguides, which was then wet-etched to form a ridge waveguide. The wet etching process included etching of the InGaAs cap layer in a $H_2O_2 : H_3PO_4 : H_2O$ $(1:1:18)$ solution, and etching of the p-type InP cladding in $HCl : H_3PO_4$ $(1:4)$ solution, stopping selectively at the top layer of the active region, creating a weakly index-guided ridge waveguide structure. After removing the SiO_2 mask in a buffered HF solution, a 3-μm-thick bisbenzocyclobutene (BCB) polymer layer spin-coated the wafer for electrical insulation. The BCB layer, after curing at 200 °C, was then etched uniformly in a CF_4–O_2-based RIE process until the top of the waveguide was exposed. Subsequent p-metal (Ti-10/Pt-20/Au-500 nm) evaporation and a bilevel resist liftoff process on top of the planarized surface resulted in p-type metal contacts with excellent metal film continuity. The fabrication concluded with lapping of the backside of the wafer to 150 μm, the n-metal (AuGeNi–Au) deposition, and a rapid thermal annealing. Fig. 1 shows the waveguide cross section after the metal deposition and the fabricated CPM laser structures with BCB insulation for the metal pads. This self-aligned process allows a straightforward and repeatable process for defining metal contacts to waveguide ridges as narrow as 2 μm without requiring critical lithography

1041-1135/$20.00 © 2005 IEEE

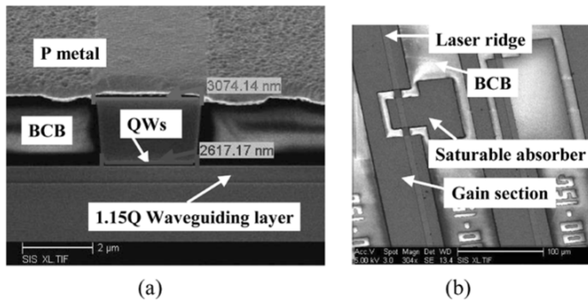

(a) (b)

Fig. 1. Scanning electron microscope photos of (a) a cross-sectional view of the wet etched laser ridge waveguide structure planarized with BCB insulation layer and (b) a top view of the CPM laser.

alignment steps. Finally for electrically isolating the gain and the SA regions, the cap layer was removed between them by selective wet etching, resulting in an isolation of approximately 2 $k\Omega$ for a 3-μm-wide waveguide across a 10-μm gap.

An insertion of the 2-μm-thick BCB insulating layer $(\varepsilon_r = 2.65)$ significantly reduces the capacitance at the SA section metal pad. The estimated capacitance is only 0.1 pF for a 100×80 μm square pad used to contact a 100-μm-wide SA section. The total capacitance including the junction capacitance of the SA section remained low, which allowed us to drive the SA section at relatively high frequency (>10 GHz) without requiring semi-insulating substrates [4] or epitaxial regrowths [2].

III. Measurement Results

Characterization of the CPM lasers started with forward-biasing the gain sections of the CPM laser using the dc needle probes. Then, a bias-Tee combines a dc reverse bias voltage and an RF modulation signal and applies it to the SA section through a ground-signal-ground (GSG) microwave coplanar probe. The CPM laser emission then coupled into a lensed fiber, passed through an optical isolator, before routing to various measurement instruments including an optical spectrum analyzer (OSA), an RF spectrum analyzer, an optical autocorrelator, and a digital sampling scope. The OSA monitored the optical spectrum showing the longitudinal modes. A 40-GHz PIN detector and a 40-GHz RF spectrum analyzer measured the electrical power spectrum. After erbium-doped fiber amplification (EDFA), the pulsed signal can be observed with a 50-GHz digital sampling scope, or with an optical autocorrelator.

We studied a 3000-μm-long CPM laser with a 100-μm-long SA section, with 10-μm gaps between the gain and SA sections. The resonant CPM frequency was estimated at 28.15 GHz, which is twice the longitudinal mode spacing. The lasing threshold was 95 mA with both the gain and the SA sections forward biased. With the gain section forward biased at 158 mA, and -2.7-V dc biasing applied to the SA section, the device operated in the passively mode-locked regime with a single intensity peak observed at 28.15 GHz in the RF power spectrum. For SHML, under the same dc biasing conditions, 26-dBm electrical modulation signal at 14.075 GHz, corresponding to the second-order $(n = 2)$ subharmonic of the CPM frequency, was applied directly to the SA section through the GSG microwave coplanar probe. The signal tip of the GSG probe contacted the SA, and the two ground tips contacted the

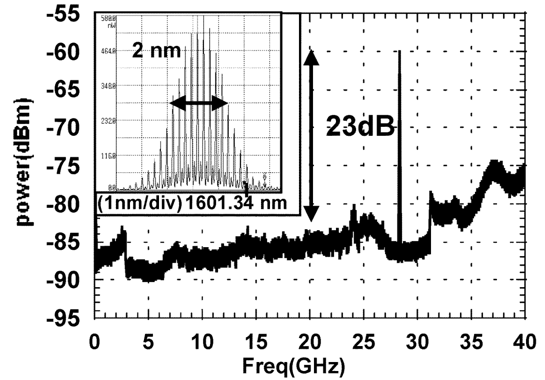

Fig. 2. Microwave power spectra of the 3000-μm CPM laser under SHML with SA-modulated with 26-dBm RF power at 14.075 GHz (23-dB AM distortion). The inset showing CPM optical spectrum.

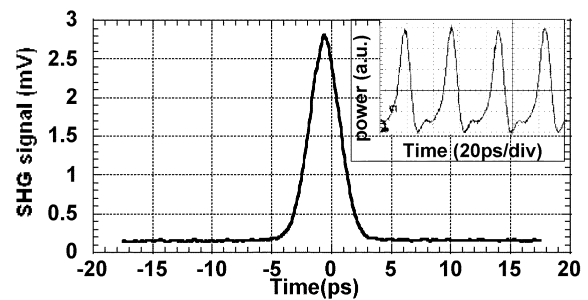

Fig. 3. Time domain autocorrelation trace of CPM output under SHML. The inset shows 50-GHz sampling scope trace synchronized with the RF source.

p-side gain sections on both sides, while the back n-side of the chip was reverse-biased relative to the p-side gain sections.

Fig. 2 shows the RF power spectrum over a 40-GHz span. A very strong intensity peak was observed at the CPM frequency, with a very weak subpeak at the drive frequency of 14.075 GHz. One concern with electrical SHML is the subharmonic driving signals introducing unwanted amplitude modulation (AM) at the drive frequencies. Here the AM modulation is 23 dB below the main peak, indicating low subharmonic distortion. This can be explained by noting that the drive frequency of 14.075 GHz was most likely far removed from the peak device modulation response at the relaxation oscillation frequency, accordingly the AM modulation effect was diminished [5]. The spectral peak at the CPM frequency under passive mode locking had 3-dB bandwidth of 1 MHz which collapsed to 20 kHz under SHML, indicating large reduction in the timing jitter. Fig. 2 (inset) shows the optical spectrum under SHML with a full-width at half-maximum of 2 nm. Fig. 3 shows the the autocorrelator trace measured utilizing second-harmonic generation with a 0.5-mm-thick $LiNbO_3$ crystal. The derived pulsewidth was 2.0 ps approximating a Gaussian pulse shape, resulting in a nearly transform-limited time-bandwidth product of 0.47.

Fig. 3 (inset) shows the laser output after EDFA amplification in the time domain using a 50-GHz sampling scope triggered with the 14.075-GHz RF modulation signal, further directly confirming CPM operation under SHML. Under the passive mode-locking condition, due to the large timing jitter, no coherent trace could be observed. With the RF modulation applied to the device, a stable 28.15-GHz pulse train can be clearly

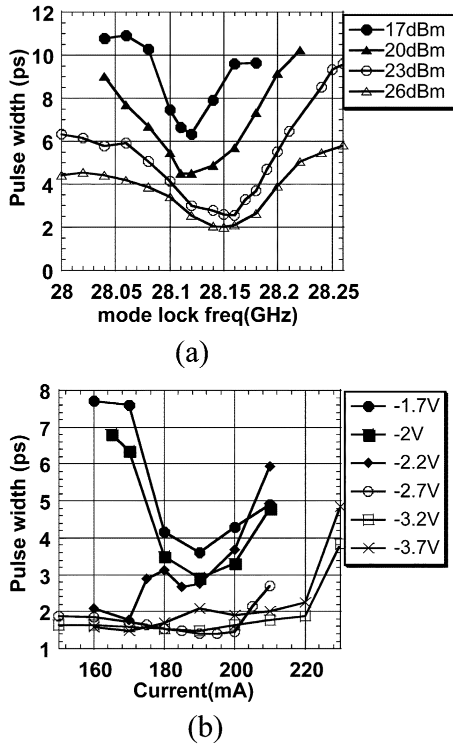

Fig. 4. Pulsewidth of a 3000-μm-long CPM laser with 100-μm-wide SA under SHML with (a) varying RF power and drive frequency, and (b) varying biasing current in the gain sections and SA reverse biasing voltage [with optimal RF biasing for minimal pulsewidth from part (a)].

observed on the sampling scope, directly confirming synchronization to the clock signal. The 50-GHz scope bandwidth only responded to the first two harmonics of the 28.15-GHz signal, producing the 12-ps-wide instrument-limited pulse and the artifact peaks between the main peaks.

We also carefully investigated the pulsewidth dependence on dc and RF biasing conditions under SHML. Fig. 4(a) shows the resulting pulsewidth as a function of actual mode-locked output frequency at different RF power levels. The pulsewidth was minimized when the mode-locking frequency nearly matched the cavity passive mode-locking frequency. The locking bandwidth also broadened with increasing RF power level with the pulsewidth saturating at 2.0 ps. With the RF biasing point optimized at the subharmonic modulation frequency of 14.075 GHz under fixed 26-dBm RF power, Fig. 4(b) shows the results of optimizing gain and dc biasing levels at the optimal RF setting. The pulsewidth dramatically decreased and the range of minimal pulsewidth widened with increasing reverse bias voltage, with a minimal pulsewidth of 1.4 ps achieved at 190 mA. This effect can be attributed to the stronger electrical field inducing faster SA carrier sweep-out and correspondingly faster SA recovery, more efficient pulse shaping [2], creating a shorter pulse. The pulse shortening effect saturated at sufficiently high field strength at -2.7-V bias at the SA. Beyond -3.7-V bias, the CPM output started to be dominated by significant self pulsation effects and stable mode locking was no longer possible. The minimal pulsewidth achieved is 1.4 ps. Efficient pulse shaping requires the physical length of the saturable absorption region to be shorter than the optical pulse [2]. The pulsewidth of our device, therefore, appears to be limited by the physical dimension of the 100-μm-wide SA and the two 10-μm gaps with a total transit time $\sim$1.4 ps. The time-bandwidth product was also nearly transform-limited at 0.46. For a given device design, we see that achieving minimal pulsewidth required careful selection of both the dc and RF biasing conditions. Such an operating condition optimization is important for optical communication system applications using the synchronized CPM lasers as ultrashort pulse sources.

IV. Conclusion

Electrical SHML operation of CPM lasers was demonstrated for the first time producing synchronized nearly transform-limited optical output pulse at 28.15 GHz with low AM distortion. Fabrication steps included very simple wet-etching-based self-aligned process developed to form ridge-waveguide CPM lasers. BCB insulation film was used to minimize contact pad capacitance and allow direct RF modulation of the SA. This simple process allows the fabrication of CPM-based inexpensive ultrafast optical sources compatible with low-cost driver electronics operating at a subharmonic of the mode-locking frequency. Careful optimization of the dc and RF biasing conditions resulted in an SA transit time-limited 1.4-ps output pulse.

References

[1] C. Ji, R. G. Broeke, Y. Du, J. Cao, N. Chubun, P. Bjeletich, F. Olsson, S. Lourdudoss, R. Welty, C. Reinhardt, P. L. Stephan, and S. J. B. Yoo, "Monolithically integrated InP based photonic chip development for O-CDMA systems," *IEEE J. Sel. Topics Quantum Electron.*, vol. 11, no. 1, pp. 66–77, Jan./Feb. 2005.

[2] Y. K. Chen and M. C. Wu, "Monolithic colliding pulse mode-locked quantum well laser," *IEEE J. Quantum Electron.*, vol. 28, no. 10, pp. 2176–2185, Oct. 1992.

[3] H. Fan, C. Wu, M. El-Aasser, N. K. Dutta, U. Koren, and A. B. Piccirillli, "Colliding pulse mode locked laser," *IEEE Photon. Technol. Lett.*, vol. 8, no. 8, pp. 972–973, Aug. 2000.

[4] H. K. Lee, V. Loyo-Maldonado, B. C. Qiu, K. L. Lee, C. Chu, S. Pinches, I. G. Thayne, A. C. Bryce, and J. H. Marsh, "Efficient direct locking of colliding pulse mode-locked lasers on semi-insulating substrate at 1.5 μm," *IEEE Photon. Technol. Lett.*, vol. 14, no. 8, pp. 1049–1051, Aug. 2002.

[5] T. Hoshida, H. F. Liu, M. Tsuchiya, Y. Ogawa, and T. Kamiya, "Subharmonic hybrid mode-locking of a monolithic semiconductor laser," *IEEE J. Sel. Topics Quantum Electron.*, vol. 2, no. 9, pp. 514–522, Sep. 1996.

[6] S. Arahira and Y. Ogawa, "480-GHz subharmonic synchronous mode locking in a short-cavity colliding-pulse mode-locked laser diode," *IEEE Photon. Technol. Lett.*, vol. 14, no. 4, pp. 537–539, Apr. 2002.

[7] H. Kurita, T. Shimuzu, and H. Yokoyama, "Experimental investigations of harmonic synchronization conditions and mechanisms of mode-locked laser diodes induced by optical-pulse injection," *IEEE J. Sel. Topics Quantum Electron.*, vol. 2, no. 3, pp. 508–513, Sep. 1996.

[8] C. Ji, N. Chubun, R. Broeke, J. Cao, Y. Du, and S. J. B. Yoo, "Synchronization of colliding pulse mode locked laser by electrical subharmonic modulation," in *Conf. Proc. 2004 IEEE LEOS Annual Meeting*, 2004, Paper WH5, pp. 527–528.